APPLICATION OF A DIGITAL IMAGE PROCEDURE TO EVALUATE MICROSTRUCTURE OF CASEINATE AND SOY PROTEIN ACID GELS

Ingrassia, Romina[1,2]; Costa, Juan P.[1,2]; Hidalgo, María E.[1,2]; Mancilla Canales, Manuel[1,2]; Castellini, Horacio[3]; Riquelme, Bibiana[1,2]; Risso, Patricia[1,2,4]

[1]Departamento de Química-Física, Facultad de Ciencias Bioquímicas y Farmacéuticas. Universidad Nacional de Rosario, Argentina
[2]Óptica Aplicada a la Biología, Instituto de Física Rosario (CONICET-UNR). Argentina
[3]Departamento de Física, Facultad de Ciencias Exactas, Ingeniería y Agrimensura, Universidad Nacional de Rosario, Argentina
[4] Facultad de Ciencias Veterinarias, Universidad Nacional de Rosario, Argentina
riquelme@ifir-conicet.gov.ar, phrisso@yahoo.com.ar

Keywords: protein acid gels; microstructure; conventional optical microscopy; image textural analysis; rheological properties

ABSTRACT

Acid gelation of proteins is commonly used in the food industry and it can be induced by the addition of glucono-δ-lactone (GDL). The aim of this work was to use textural analysis of images in order to assess possible changes in the microstructure of bovine sodium caseinate (NaCAS) and soy protein isolate (SPI) acid gels. The gelation rate of NaCAS related to the amount of GDL was evaluated. Also, the effect of the presence of NaCAS hydrolyzates obtained at different hydrolysis times by the enzyme of *Bacillus* sp. P7 was studied. Finally, SPI acid gels were evaluated in the presence of whey soy protein isolate (WSP) in different ratios. The gel images were obtained by conventional optical microscopy and texture parameters were obtained by using specific programs which were developed in Python language. Shannon entropy, smoothness, mean normalized grey level variance and uniformity were analyzed as estimators of the texture of the images obtained. Results obtained in the evaluated systems showed that these parameters were able to represent the structural changes in the gel network, as changes in size of pores or in degree of compactness. Also, these results were contrasted with rheological properties of the systems evaluated.

1. Introduction

Preference of customers for healthier industrial products having the same texture and flavour as the traditional ones, has grown over recent years. This fact accounts for the many manufacturers' growing interest in intensifying and diversifying their production lines. However, to develop these food products with the desired texture, another food constituent stabilization is needed, where proteins play a key role due to their functional and interaction properties (Foegeding, Çakır, & Koç, 2010). The use of a simplified model system provides a scientific framework, allowing prediction of the behaviour of a more complex system, and facilitating the development and formulation of new products with the desired characteristics.

Bovine milk proteins are extensively used in the food industry because of their physicochemical, nutritional and functional properties. Bovine caseins can be precipitated at pH 4.6 and may be resolubilized by increasing the pH. If the pH increase is carried out by addition of NaOH it is possible to obtain sodium caseinate (NaCAS), which is widely used in the food industry (Ennis, & Mulvihill, 2000; Mulvihill, & Fox, 1989). NaCAS are stable against heat treatment which makes them an excellent nutrient (Manski, van Riemsdijk, van der Goot, & Boom, 2007). NaCAS particles are found in aqueous solutions as individual protein molecules, oligomers (NaCAS nanoparticles) or sub micelles of caseins (Farrell, Cooke, King, Hoagland, Groves, Kumosinski et al., 1996). NaCAS assists in the texturing of different foods, for example, it is used in the industry of meat products, sausages and luncheon, due to its heat resistance, adhesiveness and ability to confer juiciness to the product.

In the food industry, proteases have been extensively used in cheese-making, bakery products, preparation of soy hydrolyzes and meat tenderized (Rao, Tanksale, Ghatge, & Deshpande, 1998; Sumantha, Larroche, & Pandey, 2006). Also, commercial proteases have

recently been used in the production of protein hydrolyzates with promising bioactive properties (Rival, Boeriu, & Wichers, 2001; Zhu, Zhou, & Qian, 2006). Particularly, enzymatic hydrolysis under mild conditions pH (6-8) and temperature (40-60°C) allows the obtention of bioactive nutritional components and improved functional properties, such as gelation, emulsification and foaming (Hartmann, & Meisel, 2007; Silva, & Malcata, 2005)

Many microorganisms produce proteases that are particularly interesting because they have well-established methods of cultivation and provide the industry with a wide variety of proteases suitable for different purposes (Gupta, Beg, & Lorenz, 2002). It has been reported that proteolytic enzymes of *Bacillus* sp. P7, isolated from the intestinal tract of a species of the Amazon basin, *Piaractus mesopotamicus*, produce high levels of extracellular proteases with biotechnological potential which can be grown on a relatively inexpensive media (Daroit, Corrêa, & Brandelli, 2009, 2011). They generate less bitterness in food protein hydrolyzates than acidic endopeptidases. Also, their low thermo tolerance is advantageous for controlling their reactivity during the production of hydrolyzates (Rao, Tanksale, Ghatge, & Deshpande, 1998).

NACAS bovine protein hydrolyzates, obtained by controlled proteolysis using an extracellular enzyme produced by *Bacillus* sp. P7 showed various biological activities: antioxidant, antibacterial, reducing power and chelating capacity (Corrêa, Hidalgo, Mancilla Canales, Risso, & Brandelli, 2011). Therefore, it is interesting to evaluate the incorporation of such hydrolyzates to a protein network which is the basis for the development of a dairy product.

Consumption of soy-based products has grown due to its beneficial effects on health and nutrition (Friedman, & Brandon, 2001). The native soy protein isolate (SPI), which has a high nutritional value, presents several functional properties. Approximately 90% of soy proteins are globulins and those that precipitate at pH 4.5 are traditionally called reserve or

storage proteins. There are two main fractions of high molecular weights referred to as globulin 7S (β-conglycinin) and globulin 11S (glycinin). They both consist of various subunits that easily associate and dissociate under different conditions of pH, ionic strength and heat treatment (Kinsella, 2001; Pearson, 1983). The protein fraction of whey soy protein isolates (WSPs), isoelectric supernatant formed during SPI preparation, consists mainly of low molecular weight components (haemagglutinin, Kunitz and Bowman-Birk antitryptic factors and enzymes such as β-amylase, lipoxygenase and urease) (Sorgentini, & Wagner, 1999). Lately, there has been further research about functional properties of soy components that are discarded or generated in the development of soymilk, tofu, isolates and concentrates. If WSP is inactivated, it has a biological value comparable to that of the storage proteins (Kishi, & Inoue, 1987).

NaCAS and SPI may form gels near their isoelectric point by the addition of GDL (Braga, Menossi, & Cunha, 2006; Campbell, Gu, Dewar, & Euston, 2009). Protein-protein interactions increase when pH decreases due to a decrease in their net charge. As a consequence, if the protein concentration is high enough, the protein aggregation occurs and the gel is formed. Protein gels are responsible for rheological/textural properties of foods, such as elasticity, resistant and hardness (Foegeding, 2007).

The deep understanding of the complex relationship between the different components in food will allow the control and/or monitoring of the micro/nanostructure. Consequently, the texture manipulation of processed foods and the formulation of new products with differential characteristics will be possible. However, the models to predict complex systems need to be continually modified to relate them more closely with the texture of food (Foegeding, Brown, Drake, & Daubert, 2003).

Changes in the gelation process rate may affect the physical properties of the resulting gel, such as texture and water holding capacity. Moreover, the addition of cosolutes modifies the conformation and the intermolecular association of biopolymers. The addition

of a component with less efficiency to be linked to hydrogen promotes polymer-polymer association, reducing the polymer-solvent interactions (Ribeiro, Rodrigues, Sabadini, & Cunha, 2004).

In order to interpret the interaction between food composition, texture, aromatization and sensory characteristics it is necessary to take into account the distribution of a phase in a multiphase system (Aguilera, 2006; Renard, van de Velde, & Visschers, 2006). The actual distribution of this phase and the gel microstructure can be investigated by means of microscopic techniques (Donato, Kolodziejcyk, & Rouvet, 2011). Among the available microscopic technique, Conventional Optical Microscopy (COM) has the advantage of requiring easier sample preparation, lower cost of equipment maintenance and a less specialized operator compared to other advanced microscopic techniques like Confocal Scanning Laser Microscopy (CSLM) or Scanning Electron Microscopy (SEM) (Guyomarc'h, Jemin, Le Tilly, Madec, & Famelart, 2009; Mellema, Walstra, van Opheusden, & van Vliet, 2002). In addition, the presence of fluorescent markers in CSLM or the sample preparation in SEM could induce alterations in the microstructure of gels. Therefore the use of a non-invasive technique as COM permits to avoid this drawback.

Image analysis provides a tool for the characterization of protein gels and this study allows us to understand how the gel network is formed and how it is affected by the processing conditions (Langton, & Hermansson, 1996). Moreover, Rodríguez-Hernández et al. (2003) showed that an increase in the elasticity of gellan systems is related to compactness and interconnectivity of the network by digital image analysis (Rodriguez-Hernández, Durand, Garnier, Tecante, & Doublier, 2003). Also, Pugnaloni et al. (2005) showed that the decrease in pore size implies an enhanced interconnectivity of the network, which increase the gel rigidity in NaCAS gels containing sucrose (Pugnaloni, Matia-Merino, & Dickinson, 2005).

To the best of our knowledge, no research has been undertaken on the use of COM to evaluate gel microstructure. Therefore, the aim of this work was to investigate changes in the microstructure of acid gels of NaCAS and SPI due to changes in gelling rate or cosolute addition by the analysis of digital images obtained by COM. Also, the relationship between the microstructure of gels and their rheological properties was analyzed.

2. Materials and methods

2.1. Materials

Bovine sodium caseinate powder, GDL and tris(hydroxymethyl)aminomethane (Tris) were purchased from Sigma-Aldrich Co. (Steinheim, Germany). HCl and NaOH were provided by Cicarelli SRL (San Lorenzo, Argentina).

NaCAS aqueous suspensions were prepared from dissolution of commercial drug in distilled water (isoionic pH) at room temperature. After concentration measurements, 0.15 g/l sodium azide was added as a bacteriostatic agent, and the solutions were stored at 4 °C. Protein concentration was determined by the Kuaye's method (Kuaye, 1994).

The SPI was prepared following the procedures outlined by Sorgentini and Wagner (1999), from defatted soy flour (Solae Latin America, Brazil), which was not heat-treated and was desolventized under mild conditions (90.7 ± 0.2 g/100g, N × 6.25) (Sorgentini, & Wagner, 1999). The WSP was prepared from the supernatant of the isoelectric precipitation (pH 4.5) of SPI proteins. It was adjusted to pH 8 and centrifuged (12,400 x g, 15 min., and 20 °C) to obtain a clarified supernatant. Later, 60 g of ammonium sulphate was added for each 100 mL of supernatant to achieve 90% saturation (Scopes, 1994; Sobral, & Wagner, 2009). The resulting precipitate was removed by centrifugation (12,400 x g, 15 min, 20°C), washed with distilled water, dialyzed against distilled water for 24 h and finally dried by lyophilization. WSP sample submitted crude protein: 99.0 ± 0.5 g/100g, N × 6.25. SPI aqueous suspensions and their mixtures with WSP were prepared to

achieve a final protein concentration of 3 g/100g stirring during 1 h at room temperature. Later, they underwent heat treatment at 100 °C for 5 min, and they were then rapidly cooled in an ice-water bath to avoid precipitation. Finally, the sample was allowed to reach room temperature.

2.2. Proteolytic enzyme production

The protease was produced by *Bacillus* sp. P7, which grew in a nutritive medium ("chicken feather") for 48 h at 30°C under constant agitation. The enzyme was obtained after the precipitation of 92 ml of the culture supernatant with 36 g of ammonium sulphate (60% saturation) at room temperature (Scopes, 1994), and liquid chromatography on Sephadex G-100. All enzyme fractions obtained formed a pool which was called P7. Proteolytic activity was measured by the azocasein method (Hummel, Schor, Buck, Boggiano, & De Renzo, 1965).

2.3. Preparation of NaCAS protein hydrolyzates

NACAS bovine samples were subjected to enzymatic hydrolysis in alkaline medium (20 10^{-3} mol/L Tris HCl pH 8) using the P7 enzyme (enzyme / substrate relation 1:50), at 45°C. Hydrolysis was stopped at different times (t_i), immediately after the addition of the enzyme (t_0), and 1, 2, 3 or 4 h after (t_1, t_2, t_3 and t_4, respectively), by thermal denaturation of the enzyme at 100°C for 15 min. Samples obtained were centrifuged 15 min at 10,400 x g and the supernatants were lyophilized and stored for their later use.

2.4. Acid gelation by GDL addition

First, the effect of gelation rate on the microstructure of NaCAS gels was tested. Solid GDL was added to a solution of NaCAS 3g/100g to achieve four systems with different ratios GDL / NaCAS concentrations (R = 0.35, 0.5, 0.7 and 1).

Second, the presence of the hydrolyzates on the microstructure of the NaCAS gels was evaluated, keeping R constant (0.5). Solid GDL was added to 5 g sample containing NaCAS 3 g/100g and NaCAS hydrolyzates 0.75 g/100g (obtained at different hydrolysis times). It should be noted that hydrolyzates showed no ability to gelling at acid pH.

Finally, texture of gels formed by mixtures of SPI and WSP were analyzed. The acid gelation process was started by addition of GDL solid on the protein solution (3 g/100g) to obtain R value of 0.35.

2.5. Conventional Optical Microscopy (COM)

After GDL addition, each sample (80 μL) was immediately placed in compartments of LAB-TEK II cells. The gelation reaction was performed in an oven at (35 ± 1) °C, keeping the humidity controlled. Gels were observed with an oil immersion objective of 100X on an inverted microscope (Union Optical) which was coupled to a digital camera (Canon Powershot A640) with a 52 mm adaptor and 9.1x zoom. Acquired images were stored in JPG format for their further analysis.

2.6. Image textural analysis

In order to process the images obtained by COM and to obtain the texture parameters, specific programs were developed in Python language. The advantage of this method is that image segmentation, commonly by subjective thresholding into binary phases, is avoided (de Bont, van Kempen, & Vreeker, 2002). The mean normalized grey-level

variance (σ^2(N)) is particularly important in texture description because it is a measure of grey-level contrast that can be used to establish descriptors of relative smoothness. Also, the following three most significant texture measures used in the literature were used in this work: Shannon entropy (S), smoothness (K) and uniformity (U) (Gonzalez, & Woods, 2001), given by:

$$S = -\sum_{i=0}^{L-1} p(N_i)\log_2(p(N_i)) \quad (1)$$

$$K = 1 - \frac{1}{1 + \frac{\sigma^2(N)}{(L-1)^2}} \quad (2)$$

$$U = \sum_{i=0}^{L-1} p^2(N_i) \quad (3)$$

where *p(Ni)* is the statistical sample frequency normalized from the grey scale and L is the highest black level. Previously, the colour images were transformed into normalized grey scale (8-bit) to achieve maximum contrast.

The value of U is maximal for an image in which all grey levels are equal (maximally uniform), and decreases from there. In contrast, S is a measurement of the variability of the histogram of grey, and is maximal for an image that contains all the shades of grey with equal probability. In general, K is an estimator of lack of scattering of the grey scale, so that when σ^2(N) tends to zero, K tends to zero too. However, K tends to 1 when fluctuations are big and σ^2(N) is maximal. In consequence, a high S value and a small U value correspond to structures in which the component particles are located in well defined sectors. On the other hand, a small S value and a high U value correspond to structures with particles dispersed throughout its volume.

In addition, the mean diameter of pores or interstices was determined through Image J software, which was obtained in pixel units. By means of a micrometer rule, it was

236 determined that 1 pixel = (0.0645 ± 0.0005) μm and, consequently, the image resolution in
237 this optical system was found to be 15.5 pixels/μm.
238
239 *2.7. Rheological properties*
240
241 Rheological properties of NaCAS/hydrolysate mixtures and SPI/WSP mixtures (3.0
242 g/100g) were determined in a stress and strain controlled rheometer TA Instruments, AR
243 G2 model (Brookfield Engineering Laboratories, Middleboro, USA) using a cone
244 geometry (diameter: 40 mm, cone angle: 2°, cone truncation: 55 mm) and a system of
245 temperature control with a recirculating bath (Julabo model ACW 100, Seelbach,
246 Alemania) connected to a Peltier plate. An amount of solid GDL according to desired R
247 was added to initiate the acid gelation. Measurements were performed every 20 s during
248 120 min with a constant oscillation stress of 0.1 Pa and a frequency of 0.1 Hz. The
249 Lissajous figures at various times were plotted to make sure that the determinations of
250 storage or elastic modulus (G′) and loss or viscous modulus (G″) were always obtained
251 within the linear viscoelastic region. The G′-G″ crossover times (t_g) of acidified systems
252 were considered as the gel times, since most studies of protein gelation have adopted this
253 criterion (Braga, Menossi, & Cunha, 2006; Curcio, Gabriele, Giordano, Calabrò, de
254 Cindio, & Iorio, 2001). pH at t_g was also determined considering the pH value at the G′-G″
255 crossover (pH_g). Also, the maximum storage modulus (G'_{max}), the maximum loss modulus
256 (G''_{max}), and loss tangent (tanδ), ratio of G''_{max} to G'_{max}, were determined. Measurements
257 were performed at least in triplicate.
258
259 *2.8. Statistical analysis*

One-way analysis of variance (ANOVA) tests were done, verifying the assumptions of normality and homogeneity of variance. Statistical significance of differences between the mean values was analyzed using the Tukey`s test.

All tests were done using R software (R-Core-Team, 2012) and level of significance was set on 0.05.

3. Results and discussion

3.1. Effect of gelation rate on NaCAS gel microstructure

Figure 1 shows the images of microstructure of NaCAS gels obtained with different R. It is possible to observe that gels showed a greater structuring at minor gelation rates (minor R). When the process is slower, the matrix of gel may carry out restructuration with formation of news interactions. Therefore, the network becomes more compact with a smaller mean diameter of the pores.

Figure 1

Table 1 shows that the mean diameter of the pores increased significantly ($p<0.05$) with GDL concentration. This result corroborates that the gel degree of compactness and the mean diameter of the pores depended on gelation rate, which increases with the amount of GDL added. This is because if the gelation process is slowly performed, the gel network can be restructured by breaking of some interactions and the forming of new ones, producing a tighter network with pores progressively smaller. Cavallieri et al. (2008) have also reported that gelation rate can affect the hardness and elasticity of the protein gels (Cavallieri, & da Cunha, 2008).

Table 1

Table 2 shows the texture descriptors of images obtained from NaCAS gels (3 g/100g) for different acidification rates at 35ºC. For this purpose, 10 images were registered for

each experimental condition. Image textural analysis showed that an increase in R caused a significative decrease of S, K and σ^2(N) and a significative increase of U. An increase in U values implies a tendency to a uniform distribution of grey levels in the image plane and a decrease in S corresponds to structures with particles dispersed throughout its volume. Thus, when R increased, the mean diameters of gel pores were bigger and the sharpness of images was lower due to the presence of NaCAS particles in the interstices leading to a poorly interconnected network.

Table 2

Results of rheological properties of NaCAS gels revealed that t_g and pH_g decreased as R increased (Table 3). Because the same amount of H^+ is needed to attain the NaCAS gelling in all samples (similar pH_g), an increase in the R value reduced t_g. A significant decrease in G'_{max} was observed when R increased from 0.5 to 0.7, as was expected according to results reported above. Although an increase in G'_{max} value at R=1 was unexpected, a clear increase of tanδ was observed, pointing out a diminution of the elastic character of gels when R increases. Similar results had been reported by Braga et al. (2006) for a lower temperature (Braga, Menossi, & Cunha, 2006).

Table 3

In conclusion, the kinetic of gel formation determines the degree of compactness of gels since it depends on the rearrangement of the inter-particular interactions during the process. When gel formation is fast, these arrangements are partial and, in consequence, the formed gels become less compact as shown in the obtained results. The importance of this result lies in the fact that the size and depth of pores are related with the elasticity of gels, which were reported by other authors using more complex procedures like CSLM and TEM (Auty, O'Kennedy, Allan-Wojtas, & Mulvihill, 2005; Pugnaloni, Matia-Merino, & Dickinson, 2005).

312 *3.2. Effect of hydrolyzate addition on microstructure of NaCAS gels*

313

314 The effect of bioactive hydrolyzate addition on NaCAS gels is shown in Fig. 2. The
315 mean diameter of the pores obtained was practically invariable (2.49 ± 0.02) μm ($p>0.05$)
316 in the presence of hydrolyzates from t_0 to t_3, indicating that the microstructure of these gels
317 did not show significant variations. Only a significant decrease in average diameter of the
318 pores in the presence of hydrolyzates t_4 was observed ((2.09 ± 0.03) μm). These values are
319 informed as mean value ± standard error.

320 The results of the analysis of textural parameters show that only the presence of the
321 hydrolyzates obtained after 4 h promoted a significant change in S and U values (Table 4).

322

323 **Figure 2**

324 **Table 4**

325

326 Results of rheological properties during gelation of NaCAS/hydrolyzate samples are
327 shown in Table 5. The results indicate that there were not any changes in the kinetic of the
328 process. Although the G'_{max} value diminishes in the presence of hydrolyzates, especially
329 with t_4 hydrolyzate, tan δ values indicate that the elastic character of gels was essentially
330 the same.

331 **Table 5**

332

333 According to these results, the degree of compactness and the microstructure of NaCAS
334 gels could not be altered by the incorporation of hydrolyzates in the NaCAS solutions.
335 These results are promising as regards the use of these hydrolyzates, which have different
336 biological activities, in the manufacture of dairy products, e.g. yoghurt-style desserts,
337 formed by the mechanism of acid-induced casein aggregation.

338

339 *3.3. Evaluation of microstructure of SPI and SPI/WSP gels*

Fig. 3 shows digital images of SPI gels in the absence (A) and in the presence of different WSP ratios (B, C and D). In these images, it is evident that the increase in WSP ratio generated gels with a more heterogeneous structure (images B at D). Previous works indicate that the mean initial size of particles from SPI/WSP mixtures increases with the WSP ratio. Also, these mixtures are more unstable and the aggregation process occurs faster (Ingrassia, 2011). Therefore, the degree of compactness of gels decreased when WSP ratio increased, probably because an increase in gelation rate that leads to a minor restructuration of the gel network.

Figure 3

The mean diameter of the pores increases significantly ($p<0.05$) when the WSP ratio increases (Table 6). These results confirm that SPI gels are less compact in the presence of WSP. Since WSP does not form gels, these changes in SPI/WSP gel mixtures could be related to a decrease in network rearrangements due to the interaction between both protein groups.

Table 6

Textural parameters obtained from acid gel images indicate that the presence of WSP induced significant changes in textural characteristics of these gels. Table 7 shows that U values were significantly lower and K, S and $\sigma^2(N)$ values were significantly higher when WSP fraction was increased. A higher S value and a smaller U value indicate that the component particles of these mesh gels are located in well defined sectors in the images.

Table 7

Rheological parameters of SPI/WSP acid gels are shown in Table 8. As mentioned above, the progressive increase of the rate of gel formation, as t_g values suggest,

diminishes the elastic character of these systems. Lower values of G'_{max} and higher values of tanδ are consistent with this observation.

Table 8

Therefore, the WSP addition modifies the SPI gel microstructures generating a network with bigger and more defined pores and with a less elastic character.

4. Conclusions

In this work a new optical technique and digital image analysis were used in order to study different acid gel microstructures. The acquisition technique of images with COM was adequate to carry out structural analysis of protein gels. Textural parameters and mean diameter of the pores obtained from these images were satisfactory related to the degree of compactness of the gel mesh. Therefore, structural changes due to gelation process conditions or the addition of cosolutes can be evaluated in an economical, sensitive and precise way.

Firstly, it may be concluded that the rate of gelling process was closely related to the final microstructure of the gel network. As this rate increases, the diameter of pores becomes bigger and the elastic character of gels was smaller. These different levels of gel microstructure were consistent with their rheological behaviors.

Secondly, the addition of hydrolyzates to the NaCAS gel matrix did not significantly alter the microstructure of these gels. On the contrary, when WSP was added to SPI dispersions it carried out to progressively weaker gels.

Finally, this procedure based in COM technique was an appropriate complement for protein gelation process analysis and for the study of the influence of different factors to develop a new food formulation with certain textural characteristics. The relationship

between textural parameters and rheological characteristics of gels was very useful in order to optimize textural characteristics of these food acid gels.

Acknowledgement

This work was supported by grants from Universidad Nacional de Rosario (UNR), Argentina. We thank the English Area of Facultad de Ciencias Bioquímicas y Farmacéuticas, UNR, for the language correction of the manuscript. We thank Pablo Sobral for advising about soy isolate preparation. We thank Hebe Bottai for the statistical analysis. Romina Ingrassia, María E. Hidalgo and Manuel Mancilla Canales are research awardees of Consejo Nacional de Investigaciones Científicas y Técnicas (CONICET), Argentina.

References

Aguilera, J. M. (2006). Seligman lecture 2005 food product engineering: building the right structures. *Journal of the Science of Food and Agriculture*, 86(8), 1147-1155.

Auty, M. A. E., O'Kennedy, B. T., Allan-Wojtas, P., & Mulvihill, D. M. (2005). The application of microscopy and rheology to study the effect of milk salt concentration on the structure of acidified micellar casein systems. *Food Hydrocolloids*, 19(1), 101-109.

Braga, A. L. M., Menossi, M., & Cunha, R. L. (2006). The effect of the glucono-[delta]-lactone/caseinate ratio on sodium caseinate gelation. *International Dairy Journal*, 16(5), 389-398.

Campbell, L. J., Gu, X., Dewar, S. J., & Euston, S. R. (2009). Effects of heat treatment and glucono-[delta]-lactone-induced acidification on characteristics of soy protein isolate. *Food Hydrocolloids*, 23(2), 344-351.

412 Cavallieri, A. L. F., & da Cunha, R. L. (2008). The effects of acidification rate, pH and
413 ageing time on the acidic cold set gelation of whey proteins. *Food Hydrocolloids*, 22(3),
414 439-448.
415 Corrêa, A. P., Hidalgo, M. E., Mancilla Canales, M., Risso, P., & Brandelli, A. (2011).
416 Hidrolizados de caseinato bovino bioactivos obtenidos por acción de una enzima
417 extracelular producida por *Bacillus* sp. P7. VI Jornadas Internacionales de Proteínas y
418 Coloides Alimentarios. Buenos Aires.
419 Curcio, S., Gabriele, D., Giordano, V., Calabrò, V., de Cindio, B., & Iorio, G. (2001). A
420 rheological approach to the study of concentrated milk clotting. *Rheologica Acta*, 40(2),
421 154-161.
422 Daroit, D. J., Corrêa, A. P. F., & Brandelli, A. (2009). Keratinolytic potential of a novel
423 *Bacillus* sp. P45 isolated from the Amazon basin fish *Piaractus mesopotamicus*.
424 *International Biodeterioration & Biodegradation*, 63(3), 358-363.
425 Daroit, D. J., Corrêa, A. P. F., & Brandelli, A. (2011). Production of keratinolytic proteases
426 through bioconversion of feather meal by the Amazonian bacterium *Bacillus* sp. P45.
427 *International Biodeterioration & Biodegradation*, 65(1), 45-51.
428 de Bont, P. W., van Kempen, G. M. P., & Vreeker, R. (2002). Phase separation in milk
429 protein and amylopectin mixtures. *Food Hydrocolloids*, 16(2), 127-138.
430 Donato, L., Kolodziejcyk, E., & Rouvet, M. (2011). Mixtures of whey protein microgels
431 and soluble aggregates as building blocks to control rheology and structure of acid induced
432 cold-set gels. *Food Hydrocolloids*, 25(4), 734-742.
433 Ennis, M. P., & Mulvihill, M. D. (2000). *Milk proteins*. Cork: Woodhead Publishing
434 Limited and CRC Press LLC.
435 Farrell, H. M., Cooke, P. H., King, G., Hoagland, P. D., Groves, M. L., Kumosinski, T. F.,
436 & Chu, B. (1996). *Particle sizes of casein submicelles and purified κ-casein*. In Parris N,

K. A., Creamer LK, Pearce J Eds. Macromolecular Interactions in Food Technology (p. 61). Washington: American Chemical Society.

Foegeding, A. E., Brown, J., Drake, M., & Daubert, C. R. (2003). Sensory and mechanical aspects of cheese texture. *International Dairy Journal*, 13(8), 585-591.

Foegeding, A. E., Çakır, E., & Koç, H. (2010). Using dairy ingredients to alter texture of foods: Implications based on oral processing considerations. *International Dairy Journal*, 20(9), 562-570.

Foegeding, E. A. (2007). Rheology and sensory texture of biopolymer gels. *Current Opinion in Colloid & Interface Science*, 12(4-5), 242-250.

Friedman, M., & Brandon, D. L. (2001). Nutritional and health benefits of soy proteins. *Journal of Agricultural and Food Chemistry*, 49, 1069-1086.

Gonzalez, J., & Woods, R. E. (2001). *Digital Image Processing*: Prentice Hall.

Gupta, R., Beg, Q. K., & Lorenz, P. (2002). Bacterial alkaline proteases: molecular approaches and industrial applications. *Applied Microbiology and Biotechnology*, 59(1), 15-32.

Guyomarc'h, F., Jemin, M., Le Tilly, V., Madec, M.-N., & Famelart, M.-H. (2009). Role of the Heat-Induced Whey Protein/κ-Casein Complexes in the Formation of Acid Milk Gels: A Kinetic Study Using Rheology and Confocal Microscopy. *Journal of Agricultural and Food Chemistry*, 57(13), 5910-5917.

Hartmann, R., & Meisel, H. (2007). Food-derived peptides with biological activity: from research to food applications. *Current Opinion in Biotechnology*, 18(2), 163-169.

Hummel, B. C. W., Schor, J. M., Buck, F. F., Boggiano, E., & De Renzo, E. C. (1965). Quantitative enzymic assay of human plasminogen and plasmin with azocasein as substrate. *Analytical Biochemistry*, 11(3), 532-547.

Ingrassia, R. (2011). Efecto de la temperatura y la adición de cosolutos sobre las propiedades estructurales y funcionales de proteínas alimentarias. Rosario: Universidad Nacional de Rosario.

Kinsella, J. E. (2001). Functional Properties of Soy Proteins. *Journal of American Oil Chemical Society*, 56, 242-258.

Kishi, K., & Inoue, G. (1987). *Soy protein in human nutrition*. International Symposium pp. 45-57).

Kuaye, A. Y. (1994). An ultraviolet spectrophotometric method to determine milk protein content in alkaline medium. *Food Chemistry*, 49(2), 207-211.

Langton, M., & Hermansson, A.-M. (1996). Image analysis of particulate whey protein gels. *Food Hydrocolloids*, 10(2), 179-191.

Manski, J. M., van Riemsdijk, L. E., van der Goot, A. J., & Boom, R. M. (2007). Importance of Intrinsic Properties of Dense Caseinate Dispersions for Structure Formation. *Biomacromolecules*, 8(11), 3540-3547.

Mellema, M., Walstra, P., van Opheusden, J. H. J., & van Vliet, T. (2002). Effects of structural rearrangements on the rheology of rennet-induced casein particle gels. *Advances in Colloid and Interface Science*, 98(1), 25-50.

Mulvihill, D. M., & Fox, P. F. (1989). *Caseins and manufactured.* In Ed., P. F. F. Development in Dairy Chemistry pp. 97-130). London & New York: Elsevier Applied Science.

Pearson, A. M. (1983). *Soy proteins*. In Hudson, B. J. F. Developments in Food Protein-2 pp. 67-108). London: Applied Science. Pub.

Pugnaloni, L. A., Matia-Merino, L., & Dickinson, E. (2005). Microstructure of acid-induced caseinate gels containing sucrose: Quantification from confocal microscopy and image analysis. *Colloids and Surfaces B: Biointerfaces*, 42(3-4), 211-217.

R-Core-Team. (2012). A language and environment for statistical computing. In Computing, R. F. f. S. Vienna, Austria.

Rao, M. B., Tanksale, A. M., Ghatge, M. S., & Deshpande, V. V. (1998). Molecular and Biotechnological Aspects of Microbial Proteases. *Microbiology and Molecular Biology Reviews*, 62(3), 597-635.

Renard, D., van de Velde, F., & Visschers, R. W. (2006). The gap between food gel structure, texture and perception. *Food Hydrocolloids*, 20(4), 423-431.

Ribeiro, K. O., Rodrigues, M. I., Sabadini, E., & Cunha, R. L. (2004). Mechanical properties of acid sodium caseinate-[kappa]-carrageenan gels: effect of co-solute addition. *Food Hydrocolloids*, 18(1), 71-79.

Rival, S. G., Boeriu, C. G., & Wichers, H. J. (2001). Caseins and Casein Hydrolysates. 2. Antioxidative Properties and Relevance to Lipoxygenase Inhibition. *Journal of Agricultural and Food Chemistry*, 49(1), 295-302.

Rodriguez-Hernández, A. I., Durand, S., Garnier, C., Tecante, A., & Doublier, J. L. (2003). Rheology-structure properties of gellan systems: evidence of network formation at low gellan concentrations. *Food Hydrocolloids*, 17(5), 621-628.

Scopes, R. K. (1994). *Salting out at high salt concentration*. In Charles R. Cantor, B. U. Protein Purification: Principles and Practice pp. 76-84). Boston: Springer.

Silva, S. V., & Malcata, F. X. (2005). Caseins as source of bioactive peptides. *International Dairy Journal*, 15(1), 1-15.

Sobral, P. A., & Wagner, J. R. (2009). Relación entre la Composición y la Actividad Antitríptica de Sueros de Soja y el Comportamiento Térmico de sus Proteínas Aisladas. *Información Tecnológica*, 20(5), 65-73.

Sorgentini, D. A., & Wagner, J. R. (1999). Comparative study of structural characteristics and thermal behavior of whey and isolate soybean proteins. *Journal of Food Biochemistry*, 23(5), 489-507.

Sumantha, A., Larroche, C., & Pandey, A. (2006). Microbiology and Industrial Biotechnology of Food-GradenProteases: A Perspective. *Food Technology and Biotechnology*, 44(2), 211-220.

Zhu, K., Zhou, H., & Qian, H. (2006). Antioxidant and free radical-scavenging activities of wheat germ protein hydrolysates (WGPH) prepared with alcalase. *Process Biochemistry*, 41(6), 1296-1302.

1. Corrigendum

Corrigendum to 'Application of a digital image procedure to evaluate microstructure of caseinate and soy protein acid gels' [LWT - Food Science and Technology 53 (2013) 120-127]

Romina Ingrassia [a,b], Juan P. Costa [a,b], María E. Hidalgo [a,b], Manuel Mancilla Canales [a,b], Horacio Castellini [c], Bibiana Riquelme [a,b], Patricia Risso [a,b,d,*]

[a] Departamento de Química-Física, Facultad de Ciencias Bioquímicas y Farmacéuticas, Universidad Nacional de Rosario, Argentina
[b] Óptica Aplicada a la Biología, Instituto de Física Rosario (CONICET-UNR), Argentina
[c] Departamento de Física, Facultad de Ciencias Exactas, Ingeniería y Agrimensura, Universidad Nacional de Rosario, Argentina
[d] Facultad de Ciencias Veterinarias, Universidad Nacional de Rosario, Argentina

---

The authors regret < The protease produced by Bacillus sp. P7 was isolated during a research stay directed by Dr. Adriano Brandelli at the Instituto de Ciência e Tecnologia de Alimentos, Universidade Federal de Rio Grande do Sul, as part of a bilateral cooperation project. >.

The authors would like to apologise for any inconvenience caused.

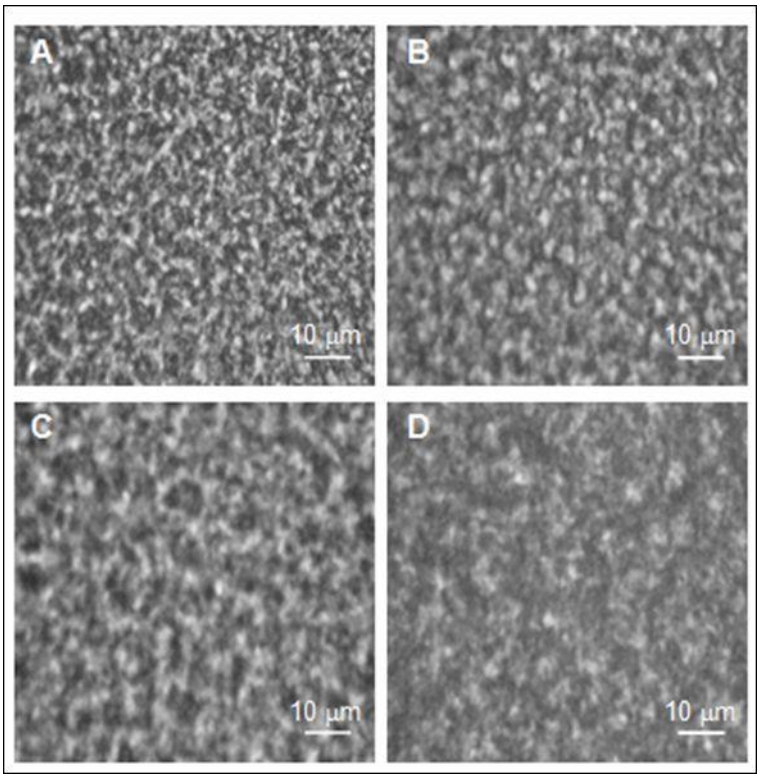

Fig. 1. Digital images of the microstructure of NaCAS gels obtained with different ratios GDL / NaCAS concentrations (R): A) 0.35; B) 0.5; C) 0.7 and D) 1. NaCAS concentration: 3 g/100g, T= 35 ºC.

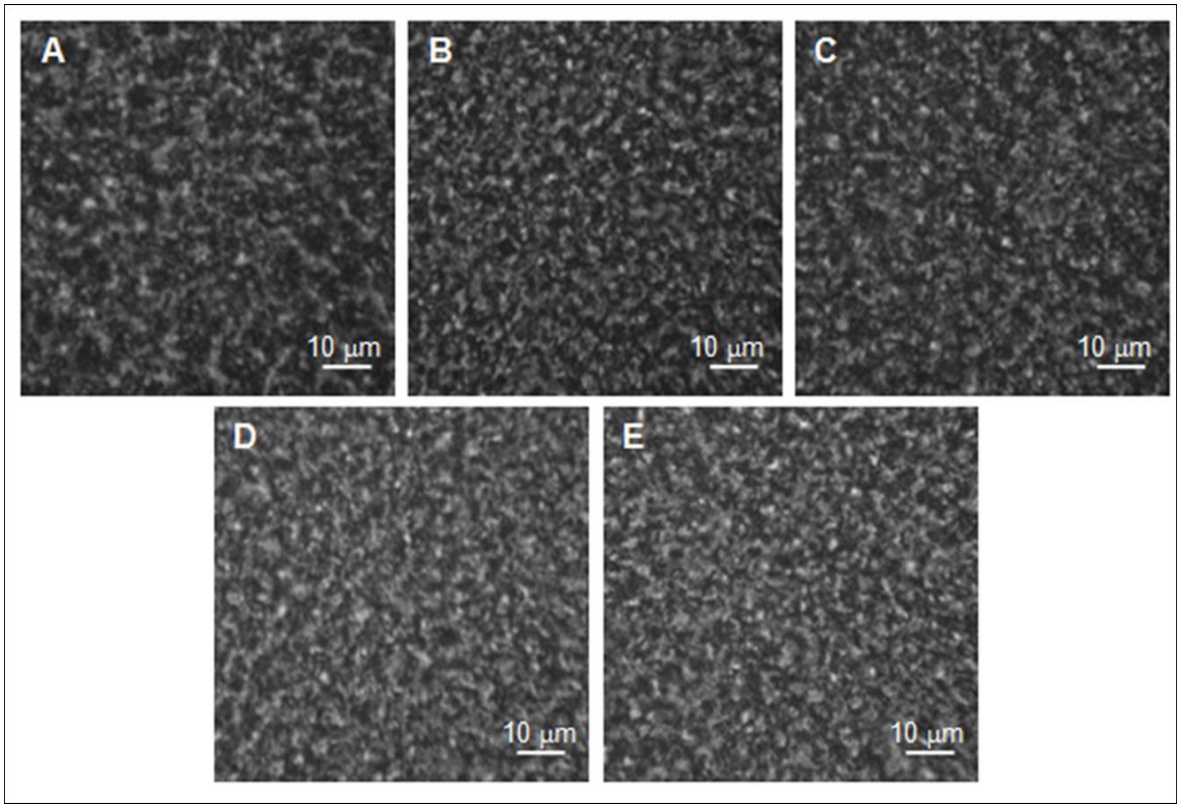

Fig. 2. Digital images of the microstructure of NaCAS/hydrolyzate acid gels. Hydrolyzates were obtained by hydrolysis with protease P7 at different hydrolysis time (t_i): A) t_0; B) t_1; C) t_2, D) t_3 and E) t_4. NaCAS concentration: 3 g/100g, hydrolyzate concentration: 0.75 g/100g, R= 0.5 and T= 35 ºC.

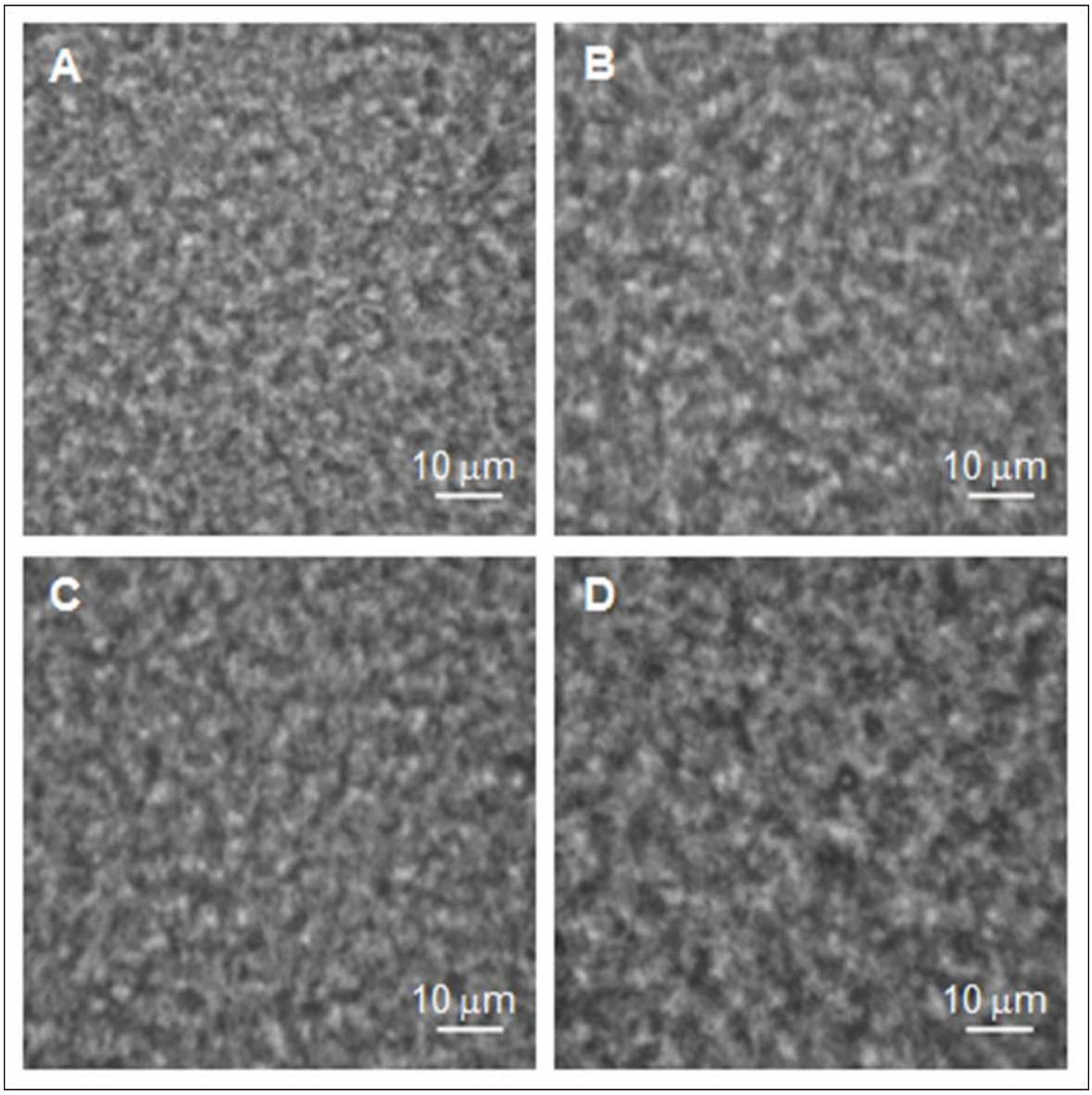

Fig. 3. Digital images of the microstructure of acid gels of A) soy protein isolate (SPI) 3 g/100g and its mixtures with whey soy protein isolate (WSP) (g/100g SPI/g/100gWSP): B) 2.25/0.75, C) 1.5/1.5 and D) 0.75/2.25. Ratio GDL / protein concentrations (R) = 0.35 and T= 35°C.

Table 1

Mean diameters of the pores of NaCAS gels obtained at different ratios GDL / NaCAS concentrations (R). NaCAS concentration: 3 g/100g, T: 35 ºC.

R	Mean diameter of pores
0.35	6.54 ± 0.07[a]
0.5	7.80 ± 0.20
0.7	8.40 ± 0.30
1	9.30 ± 0.20

[a] Mean value ± standard deviation ($p<0.05$)

Table 2

Textural parameters obtained from digital images of NaCAS gels at different ratios GDL / NaCAS concentrations (R): Shannon entropy (S), smoothness (K), uniformity (U), and mean normalized grey level variance ($\sigma^2(N)$). NaCAS concentration: 3 g/100g, T= 35 ºC.

R	S	K ($x10^{-3}$)	U ($x10^{-3}$)	$\sigma^2(N)$	ANOVA for S	ANOVA for K	ANOVA for U	ANOVA for $\sigma^2(N)$
0.35	6.9 ± 0.1[a]	20.8 ± 2.0	9.5 ± 0.7	1400 ± 100	C[b]	C	A	C
0.5	6.8 ± 0.1	17.7 ± 0.6	10.3 ± 0.6	1170 ± 40	CB	B	AB	B
0.7	6.5 ± 0.2	16.0 ± 1.4	12.8 ± 2.3	1100 ± 100	B	B	B	B
1	6.1 ± 0.2	11.9 ± 1.0	17.3 ± 2.2	780 ± 60	A	A	C	A

[a] Mean value ± standard deviation ($p<0.05$)

[b] Within a column, different letters denote mean value of parameter K, S, U or $\sigma^2(N)$ significantly different among the values of R (A stands for the lowest, B for medium value and C for the highest value, respectively)

Table 3

Gel times (t_g), pH at onset of gelation (pH_g), maximum storage modulus (G'_{max}) and tanδ for formulations containing NaCAS 3 g/100g at different ratios GDL / NaCAS concentrations (R). T= 35 ºC.

R	t_g (min)	pH_g	G'_{max}	tanδ
0.5	14.03 ± 0.01[a]	4.97 ± 0.02	79 ± 6	0.24 ± 0.01
0.7	13.13 ± 0.02	4.99 ± 0.01	44 ± 3	0.29 ± 0.02
1	11.03 ± 0.01	5.02 ± 0.01	71 ± 4	0.32 ± 0.01

[a] Mean value ± standard deviation ($p<0.05$)

Table 4

Textural parameters obtained from digital images of NaCAS/hydrolyzate acid gels in function of hydrolysis time (t_i): Shannon entropy (S), smoothness (K), uniformity (U), and mean normalized grey level variance ($\sigma^2(N)$). NaCAS concentration: 3 g/100g, hydrolyzate concentration: 0.75 g/100g, R= 0.5 and T= 35 ºC.

R	S	K ($x10^{-3}$)	U ($x10^{-3}$)	$\sigma^2(N)$	ANOVA for S	ANOVA for K	ANOVA for U	ANOVA for $\sigma^2(N)$
0.35	6.9 ± 0.1[a]	20.8 ± 2.0	9.5 ± 0.7	1400 ± 100	C[b]	C	A	C
0.5	6.8 ± 0.1	17.7 ± 0.6	10.3 ± 0.6	1170 ± 40	CB	B	AB	B
0.7	6.5 ± 0.2	16.0 ± 1.4	12.8 ± 2.3	1100 ± 100	B	B	B	B
1	6.1 ± 0.2	11.9 ± 1.0	17.3 ± 2.2	780 ± 60	A	A	C	A

[a] Mean value ± standard deviation ($p<0.05$)

[b] Within a column, different letters denote mean value of parameter K, S, U or $\sigma^2(N)$ significantly different among the values of R (A stands for the lowest, B for medium value and C for the highest value, respectively)

Table 5

Gel times (t_g), pH at onset of gelation (pH_g), maximum storage modulus (G'_{max}) and tanδ for NaCAS/hydrolyzate acid gels at different hydrolysis times (t_i). NaCAS concentration: 3 g/100g, hydrolyzate concentration: 0.75 g/100g, R= 0.5 and T= 35 ºC.

t_i	t_g (min)	pH_g	G'_{max}	tanδ
t_0	22.4 ± 0.1[a]	4.92 ± 0.02	57 ± 6	0.36 ± 0.01
t_1	22.4 ± 0.2	4.97 ± 0.03	54 ± 3	0.34 ± 0.02
t_2	22.9 ± 0.2	4.93 ± 0.01	48 ± 5	0.33 ± 0.02
t_3	25.9 ± 0.5	4.91 ± 0.01	40 ± 4	0.32 ± 0.01
t_4	23.7 ± 0.3	4.93 ± 0.01	27 ± 5	0.31 ± 0.01

[a] Mean value ± standard deviation ($p<0.05$)

Table 6

Mean pore diameters of acid gels obtained from soy protein isolate (SPI)/ whey soy protein isolate (WSP) mixtures (3g/100g total protein). Ratio GDL / protein concentrations (R) = 0.35 and T= 35°C.

SPI/WSP	Mean diameter of pores
3/0	1.9 ± 0.3[a]
2.25/0.75	2.3 ± 0.5
1.5/1.5	2.6 ± 0.5
0.75/2.25	3.5 ± 0.8

[a] Mean value ± standard deviation ($p<0.05$)

Table 7

Textural parameters obtained from digital images of acid gels obtained from SPI/WSP mixtures (3 g/100g total protein) in function of WSP concentration: Shannon entropy (S), smoothness (K), uniformity (U), and mean normalized grey-level variance ($\sigma^2(N)$). R= 0.35 and T= 35 ºC.

SPI/WSP	S	K (x10^{-3})	U (x10^{-3})	$\sigma^2(N)$	ANOVA for S	ANOVA for K	ANOVA for U	ANOVA for $\sigma^2(N)$
3/0	6.07 ± 0.08[a]	13.3 ± 0.7	17.4 ± 0. 6	880 ± 50	A[b]	A	C	A
2.25/0.75	6.30 ± 0.07	15.8 ± 0. 6	14.4 ± 0.8	1060 ± 40	B	B	A	B
1.5/1.5	6.28 ± 0.03	15.6 ± 1.0	15.3 ± 1.0	1030 ± 70	B	B	B	B
0.75/2.25	6.41 ± 0.03	17.2 ± 1.2	13. 6 ± 0.3	1110 ± 80	C	C	A	C

[a] Mean value ± standard deviation ($p<0.05$)

[b] Within a column, different letters denote mean value of parameter K, S, U or $\sigma^2(N)$ significantly different among the values of SPI/WSP (A stands for the lowest, B for medium value and C for the highest value, respectively)

Table 8

Gel times (t_g), pH at onset of gelation (pH_g), maximum storage modulus (G'_{max}) and tanδ for soy protein isolate (SPI)/ whey soy protein isolate (WSP) mixtures (3g/100g total protein). Ratio GDL / protein concentrations (R) = 0.35 and T= 35°C

SPI/WSP	t_g (min)	pH_g	G'_{max}	tanδ
3/0	16 ± 1[a]	5.64 ± 0.04	389 ± 3	0.188 ± 0.006
2.25/0.75	10.4 ± 0.5	5.71 ± 0.07	275 ± 6	0.199 ± 0.006
1.5/1.5	6.0 ± 0.2	5.8 ± 0. 1	184 ± 30	0.212 ± 0.007
0.75/2.25	5 ± 1	5.76 ± 0.02	44 ± 2	0.241 ± 0.003

[a] Mean value ± standard deviation ($p<0.05$)

Highlights:

- We evaluate gel microstructure changes with an economical and sensitive technique
- Pore diameters and the elasticity of gels depend on the rate of gelling process
- Hydrolyzates addition not significantly alter sodium caseinate gel microstructure
- Whey soy protein addition results in soy protein isolate weaker gels